Journal of Power Sources 206 (2012) 357–366

Contents lists available at SciVerse ScienceDirect

Journal of Power Sources

journal homepage: www.elsevier.com/locate/jpowsour

Method to deduce the critical size for interfacial delamination of patterned electrode structures and application to lithiation of thin-film silicon islands

Hamed Haftbaradaran[a], Xingcheng Xiao[b], Mark W. Verbrugge[b], Huajian Gao[a,*]

[a] School of Engineering, Brown University, Providence, RI 02912, USA
[b] General Motors Global Research & Development Center, Chemical Sciences and Materials Systems Laboratory, 30500 Mound Road, MC: 480-106-224, Warren, MI 48090, USA

ARTICLE INFO

Article history:
Received 3 September 2011
Received in revised form 12 January 2012
Accepted 14 January 2012
Available online 24 January 2012

Keywords:
Delamination
Interface
Patterned thin films
Silicon negative electrodes

ABSTRACT

Recent experiments have suggested that there is a critical size for patterned silicon (Si) thin film electrodes for delamination from a current collector during lithiation and delithiation cycling. However, no existing theories can explain this phenomenon, in spite of its potential importance in designing reliable electrodes for high-capacity lithium-ion batteries. In this study, we show that the observed delamination size effect can be rationalized by modeling thin film delamination in the presence of large scale interfacial sliding. A method is proposed to deduce the critical size for delamination based on the critical conditions for the nucleation and growth of edge or center cracks at the film-substrate interface under plane strain or axisymmetric conditions. Applications to lithiation of thin-film Si islands give results in excellent agreement with experimental observations.

1. Introduction

Mechanical degradation such as fracture and delamination of electrodes due to lithiation and delithiation has been widely recognized as one of the main causes for the short cycle life of high-capacity lithium-ion (Li-ion) batteries [1,2]. For such applications, silicon (Si) holds the maximum theoretical charge capacity and has been intensely studied as one of the most promising negative electrode materials. However, mechanical degradation has been frequently reported in Si electrodes fabricated in various forms of thin films [2–7], nanowires [8,9], and composite nano-structures [10]. It has been shown that 250 nm thick Si films on copper (Cu) foils exhibit near theoretical charge capacity for a limited number of cycles, but the capacity fades drastically upon further cycling due to fracture and delamination [7]. Numerous studies have been devoted to improving the electrochemical and mechanical stability/performance of Si electrodes by reducing the size of Si particles below a critical fracture-resistant size [6], enhancing adhesion between thin film electrodes and substrate [11], avoiding formation of crystalline $Li_{15}Si_4$ phase which is associated with formation of high internal stresses [12,13], and reducing the film thickness to achieve higher cycling rates [14]. For thin-film Si electrodes deposited on substrates, it is worth pointing out that, although the lithiation and delithiation cycling may generate microcracks through the film thickness, the fractured film can still serve as the active material as long as it can remain adhered to the current collector. In fact, through-the-thickness cracks in such systems can alleviate diffusion-induced stresses by facilitating volume changes associated with Li insertion/extraction. Therefore, while fracture in thin film electrodes partly decreases their capacity due to the formation of solid-electrolyte interphase (SEI) layers at newly created cracked surfaces, film delamination is a far more critical issue to capacity fading in such electrodes.

The present paper is aimed to present a method to deduce the critical size for interfacial delamination of thin film electrodes by examining the critical conditions for the nucleation and propagation of interfacial cracks at the film–substrate interface under plane strain or axisymmetric conditions. The motivation for this study has come from the following experimental observations on the delamination behaviors of Si thin film electrodes which have been reported in our recent paper [15] but remains unexplained to this date. First, it was observed that a continuous Si thin film with thickness of 100 nm exhibits through-the-thickness cracks with spacing in the range of 5–10 μm due to lithiation and delithiation. Next, a set of experiments was performed to investigate the fracture behaviors of patterned Si thin film square islands on Cu with the same film thickness of 100 nm but 3 different lateral dimensions: 7 μm × 7 μm, 17 μm × 17 μm and 40 μm × 40 μm. Scanning electron microscope images then showed that the 7 μm × 7 μm Si islands stayed well adhered to the substrate, while a fraction of the 17 μm × 17 μm islands and all of the 40 μm × 40 μm islands peeled off the substrate after 30 charge-discharge cycles. Therefore, a critical island size seems to exist in the order of 10–20 μm for interfacial delamination of patterned thin films with thickness

* Corresponding author.
E-mail address: Huajian_Gao@brown.edu (H. Gao).

0378-7753/$ – see front matter © 2012 Elsevier B.V. All rights reserved.
doi:10.1016/j.jpowsour.2012.01.097

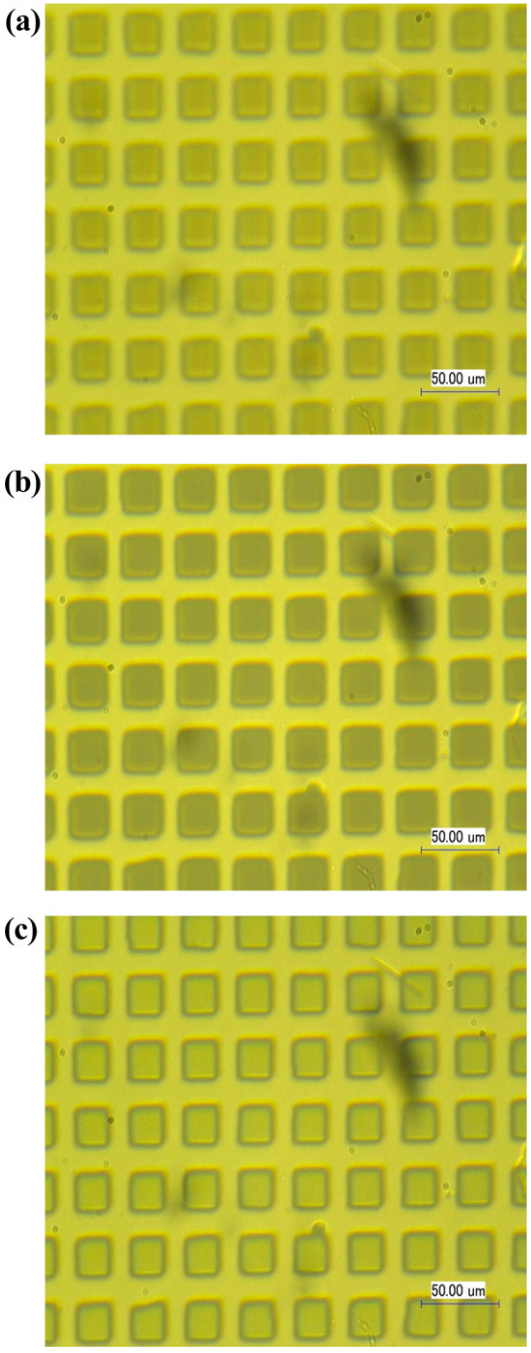

Fig. 1. Micrographs demonstrating lateral expansion and contraction of Si islands on Ti current collector due to lithiation and delithaition. (a) As-deposited 17 μm × 17 μm Si islands; (b) lateral dimensions of the Si islands expand by about 30% parallel to the substrate, demonstrating sliding along the interface; (c) Si islands return to their original size after delithiation. The scale bar is 50 μm (after [21]).

of 100 nm. The existing theories of interfacial delamination [16–20] simply cannot explain why the 100 nm thick islands exhibit such size-dependent delamination behavior in the size range nearly two orders of magnitude beyond the film thickness. In the present study, we show that this effect can only be rationalized by considering thin film delamination in the presence of large scale interfacial sliding. Fig. 1a shows an array of 17 μm × 17 μm Si islands deposited on a titanium (Ti) current collector. Upon lithiation, it was observed that the Si islands underwent about 30% of lateral expansion parallel to the substrate, as demonstrated in Fig. 1b. Fig. 1c shows that the same islands were able to shrink back to their original size upon deilthiation. These in-plane expansion and contraction of Si islands indicate large scale sliding along the film–substrate interface [21]. By accounting for the effect of interfacial sliding, we will develop a method to deduce the critical size for interfacial delamination in patterned electrode structures by examining the critical conditions for the nucleation and propagation of edge or center cracks at the film-substrate interface under plane strain or axisymmetric conditions.

It is worth pointing out that the present work can be regarded as part of a series of studies on patterned thin film electrodes [15,21,22]. In a previous study [15], we have already proposed a shear lag model which, by accounting for interfacial sliding or substrate yielding, explains the experimentally observed fracture spacing in continuous Si thin films. This model, when applied to patterned Si thin film islands, would imply that there is substantial sliding at the film–substrate interface and that it is possible to choose the island size such that the maximum stress in the island stays below the flow stress of lithiated Si, in which case the island would remain elastic during Li insertion/extraction [22]. The same model has been successfully used to model stress evolution in patterned thin film islands on Ti substrates, with results in excellent agreement with experiments [22]. According to these experiments, the interfacial sliding strength has been estimated at about 40 MPa between lithiated Si and Cu [15], and about 10 MPa between lithiated Si and Ti [21,22], which are comparable with direct experimental measurements of interfacial sliding resistance in other similar kinds of material systems [23]. In spite of these progresses, the anomalous critical size for interfacial delamination in thin-film Si electrodes during lithiation and delithiation has not been explained and, therefore, the question of what factors control the delamination of electrodes from the current collector still remains open. In the present manuscript, we shall attempt to close this gap by investigating the delamination behaviors of patterned thin film electrodes in the presence of large scale interfacial sliding.

2. Theories of fracture and delamination

Theories of fracture mechanics and diffusion-induced stresses have been employed to model fracture of electrodes, with results suggesting the existence of a critical size and charging rate below which fracture becomes impossible [6,24–31]. A widely accepted result is that sufficiently thin electrodes are resistant against fracture in the thickness direction.

Delamination of thin films on substrate has been widely studied in the literature [16–20]. An assumption commonly made in modeling delamination of thin films on substrate is that the film is well-bonded to the substrates with no interfacial sliding [16–20]. Under plane strain conditions, a well-known result is that the energy release rate associated with an edge delamination crack reaches a steady-state value of $G_0 = (1-\nu^2)\sigma_f^2 h/2E$ as soon as the crack size becomes comparable to or larger than the film thickness h, where σ_f is the stress in the film, and E and ν are the Young's modulus and Poisson's ratio of the film, respectively [16,19]. However, when the interfacial sliding strength is much smaller than the stress in the film, as is the case expected for a Si electrode on a current collector, a large scale interfacial sliding zone would be expected near the edges of the film. If the length of the film is larger than the size of the sliding zone, a delamination crack would grow in a steady state manner as soon as the crack size is larger than the film thickness. In this state, the energy release rate is independent of the crack size, and there is no size effect (Fig. 2a). On the other hand, if the interfacial sliding zones from the island edges are so large that they extend over the entire island (Fig. 2b), a strong delamination size effect would emerge over the size scale associated with the size of the sliding zones, rather than the film thickness. The shaded area

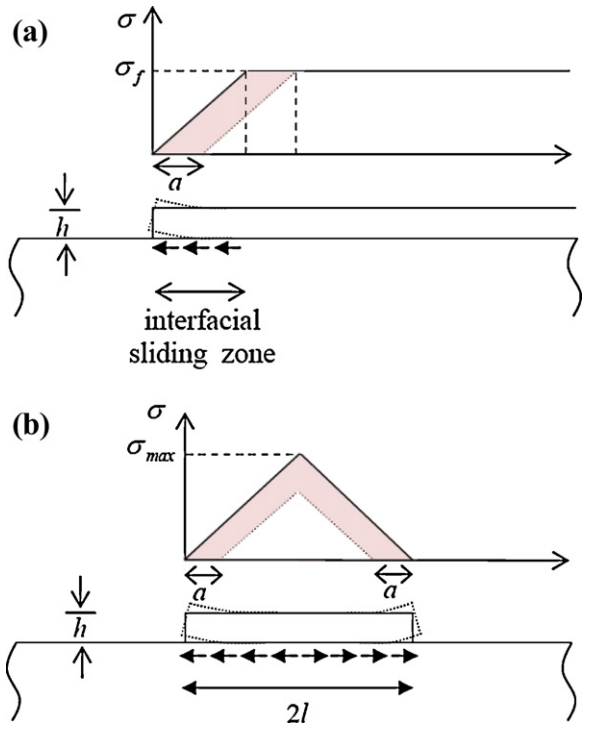

Fig. 2. Schematic of an edge delamination crack in a thin film on substrate in the presence of large scale interfacial sliding. (a) The crack grows in a steady state manner when the film width is much larger than the interfacial sliding zone at the film edge. (b) The interfacial delamination becomes dependent on the island size as the sliding zones from island edges overlap. In this case, the energy release rate for interfacial delamination is expected to decrease as the island size is reduced.

in Fig. 2b shows the region in which stress is released as two edge cracks nucleate and grow to a size a. It is evident that the shaded area in Fig. 2b would shrink as the island size is reduced, and hence the energy release rate is expected to decrease. This is in contrast to the case shown in Fig. 2a, which corresponds to a relatively large island size compared to the size of the sliding zones, leading to a size-independent energy release rate. Since the size of the interfacial sliding zones also determines the length scale over which the normal stress in the film reaches its maximum value, the size effects associated with interfacial sliding immediately suggests an explanation for the experimentally observed correlation between the fracture spacing in a continuous Si thin film and the critical size for interfacial delamination in patterned Si islands. Therefore, interfacial sliding between lithiated Si electrodes and substrate, which can occur on a much larger length scale than the film thickness, is a key to deducing the critical size for interfacial delamination in patterned Si electrodes. The reason that the existing theories of interfacial delamination [16–20] cannot explain the experimental observation that Si islands with thickness of 100 nm and length of 7 μm stayed well adhered on the substrate while those with the same thickness but length of 40 μm delaminated away can be attributed to the fact that the assumption of well-bonded and non-slipping interface, while applicable to many conventional thin film-substrate systems, no longer holds in the case of lithiation of high-capacity electrodes.

In the following, we will deduce the critical size for interfacial delamination by detailed plane strain and axisymmetric analysis of potential nucleation and growth of edge and center interfacial cracks in the presence of large scale interfacial sliding. We will take advantage of the symmetry in the problem to simplify the analysis. Furthermore, we will treat the edge and center cracks separately, since their coexistence would decrease the elastic energy release rate in the islands as the driving force for crack nucleation and

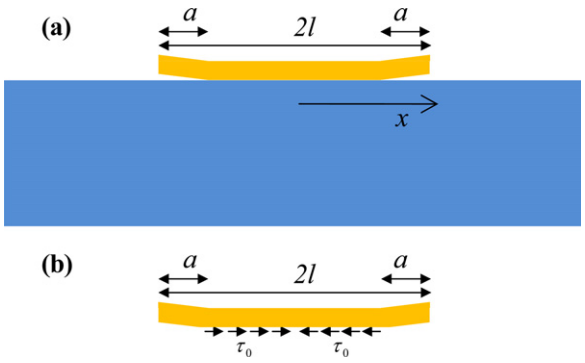

Fig. 3. Schematic of (a) a Si island on substrate with edge delamination cracks and (b) a free-body diagram of the island.

growth. The interface between the island and substrate is assumed to be well-bonded under small shear tractions but interfacial sliding is allowed as soon as the interfacial shear stress reaches a critical value τ_0. It is also assumed that the sliding follows a perfectly plastic response so that the interfacial shear stress never exceeds the sliding strength τ_0. The immediate consequence of this behavior is that the interfacial sliding zones start to develop at the edges of the film and spread toward the center of the island. Once they spread to the center of the island, the entire island would be sitting on top of a slippery surface and can freely expand upon further lithiation. This is the case as long as deformation within the island remains elastic, i.e. the maximum stress in the island does not exceed the flow stress of lithiated Si.

3. Nucleation and growth of edge delamination cracks in the presence of large scale interfacial sliding

In this section, we will investigate the nucleation and growth of edge delamination cracks in a Si island with interfacial sliding zones spreading over the entire island. For simplicity, it will be assumed that the film is thin enough that variation of stress in the thickness direction can be neglected.

3.1. Plane strain analysis

Consider a Si island of length $2l$ and thickness h on a substrate, with edge delamination cracks of size a at the interface at both edges of the island, as shown in Fig. 3. Assuming that the interfacial sliding zones from both edges of the island overlap, the axial stress distribution in half of the patch would be given as

$$\sigma_{xx} = \frac{\tau_0}{h}\begin{cases} l-a-x & l-a>x>0 \\ 0 & l>x>l-a \end{cases}, \tag{1}$$

where x is distance from the center of island. The total elastic energy stored, per unit out-of-plane length, in half of the island is obtained as

$$U_{el} = \int_0^{+l} \frac{1-\nu^2}{2E}\sigma_{xx}^2\, dx = \frac{(1-\nu^2)\tau_0^2}{2hE}\frac{1}{3}(l-a)^3, \tag{2}$$

where E and ν are, respectively, the Young's modulus and Poisson's ratio of the film. To investigate the criterion for crack growth, we first note that the elastic energy release rate G is

$$G = -\frac{dU_{el}}{da} = \frac{(1-\nu^2)\tau_0^2}{2hE}(l-a)^2. \tag{3}$$

Interface delamination is accompanied with formation of new surfaces which increases the total free energy of the system. Denoting

the interface fracture energy (toughness) by Γ, the total surface energy of the system U_{surf} increases at the rate of

$$\frac{dU_{surf}}{da} = \Gamma. \tag{4}$$

The Griffith condition for crack growth is that the elastic energy release rate must exceed the growth rate of surface energy, that is $G > dU_{surf}/da$, which yields

$$(l-a) > \sqrt{\frac{2hE\Gamma}{(1-\nu^2)\tau_0^2}}. \tag{5}$$

For an initially crack-free interface, i.e. $a = 0$, Eq. (5) suggests that edge delamination at the interface is only favorable for islands larger than a critical length,

$$l > l_{cr,nuc} = \sqrt{\frac{2hE\Gamma}{(1-\nu^2)\tau_0^2}}. \tag{6}$$

In this case, nucleation of edge interfacial cracks decreases the total free energy of the system. Fig. 4a shows the variations of the elastic energy rate vs. the crack length a, where the dimensionless parameters $\tilde{U}_{el} = 2hEU_{el}/(1-\nu^2)\tau_0^2 l^3$ and $\tilde{U}_{surf} = 2hEU_{surf}/(1-\nu^2)\tau_0^2 l^3$ have been introduced. As shown in this figure, the elastic energy release rate associated with crack growth decreases with the crack length, while surface energy rises at a constant rate. Therefore, the crack is expected to be arrested at a residual length a_{arr}. This residual length can be obtained from the condition that the total released elastic energy of the system prior to arresting has been completely consumed to create new surfaces, and thus there is no more energy available for crack to grow, i.e.

$$U_{el}(a=0) - U_{el}(a=a_{arr}) = U_{surf}(a=a_{arr}) - U_{surf}(a=0). \tag{7}$$

Straightforward manipulation shows that

$$a_{arr} = \frac{1}{2}\left(3l - \sqrt{3(4l_{cr,nuc}^2 - l^2)}\right). \tag{8}$$

Fig. 4b shows how a_{arr}/l varies with $l/l_{cr,nuc}$. One can easily verify that at this crack length, the elastic energy release rate becomes less than the surface energy growth rate. An interesting case happens when $a_{arr} \geq l$, corresponding to the scenario when the two edge cracks would grow all the way to the center of the island. In this case, the island will peel off from the substrate. It can be shown that this is the case only when the length of the island is larger than a critical length associated with full delamination,

$$l \geq l_{cr,del} = \sqrt{3} l_{cr,nuc} = \sqrt{\frac{6hE\Gamma}{(1-\nu^2)\tau_0^2}}. \tag{9}$$

To further elucidate the delamination mechanisms, Fig. 4c shows changes in the dimensionless elastic and surface energies of the system, i.e. $|\Delta\tilde{U}_{el}| = \tilde{U}_{el}(0) - \tilde{U}_{el}(a)$, and $\Delta\tilde{U}_{surf} = \tilde{U}_{surf}(a) - \tilde{U}_{surf}(0)$, for various island sizes, as a function of the crack length. It can be seen that, in the critical case of $l = l_{cr,del} = \sqrt{3} l_{cr,nuc}$, marked by a solid circle in Fig. 4c, the total released elastic energy is just enough to drive the crack all the way to the center. As is evident from the same figure, larger islands with $l = 2l_{cr,nuc} > l_{cr,del}$ have even higher elastic energy and will delaminate away. However, for a shorter island with $l = 1.5 l_{cr,nuc} < l_{cr,del}$, the surface energy grows beyond the total elastic energy available in the island, indicating that the full delamination is impossible, in consistence with Eq. (9). In the latter case, the ultimate length of the arrested crack can be obtained via Eq. (8).

A couple of remarks are worth making at this point. While in the above analysis we have considered a pair of symmetrical edge interfacial cracks, one can verify through straightforward analysis that consideration of a single edge crack does not change the results. Furthermore, in the present analysis, we have ignored the elastic energy stored in the substrate. Treating substrate as an elastic half-plane, a dimensional analysis would reveal that the ratio of elastic energy stored in the substrate to that in the film scales as $Eh/E_s(l-a)$, where E_s is the Young's modulus of the substrate. Therefore, while our analysis is exact for the case of a rigid substrate, it remains valid even for an elastic substrate as long as the length of the island in contact with the substrate is much larger than the thickness of the island. This is indeed the case for patterned Si thin film electrodes with length on the order of tens of micrometers and thickness of a few hundred nanometers. As the island loses its contact with the substrate along the interface with contact area shrinking to a size comparable to the film thickness, the above assumption starts to break down. However, when this happens, the island can be considered as having effectively detached from the substrate.

For further physical insights, some numerical estimates of the critical length scales for interfacial delamination would be helpful.

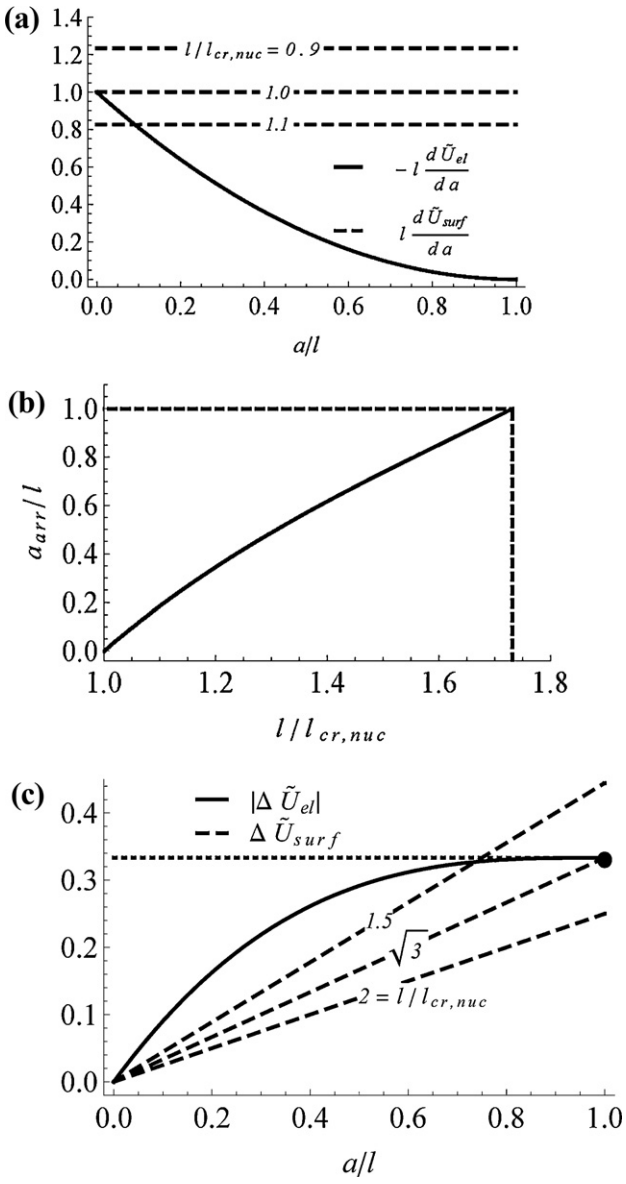

Fig. 4. Plane strain analysis of interfacial delamination of a Si island on substrate. (a) Elastic energy release rate and surface energy growth rate vs. crack length for various island sizes; (b) length of the arrested edge crack as a function of the island size; (c) changes in the elastic energy and surface energy as a function of the crack length for different island sizes.

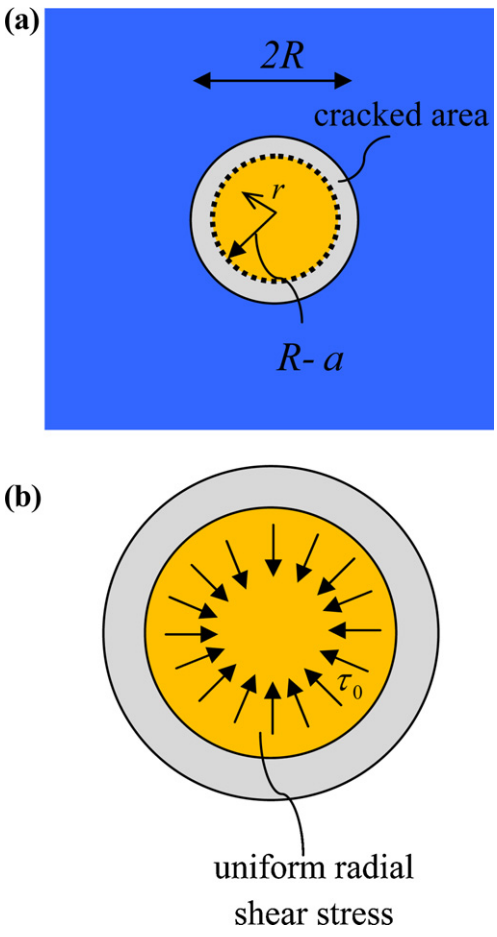

Fig. 5. Schematic of (a) a Si circular island on substrate with an annular edge crack and (b) a free-body diagram of the island.

For a 100 nm thick Si patch with $E = 40$ GPa and $\nu = 0.22$ (for lithiated Si [32]), $\tau_0 \approx 10$ MPa (for patterned Si thin films [21,22]), and a typical value of 1 J/m^2 for the interface energy Γ, the critical island sizes for crack nucleation and full delamination are estimated to be $2l_{cr,nuc} \approx 18.3$ μm and $2l_{cr,del} \approx 31$ μm, respectively, corresponding to maximum stresses of 0.92 GPa and 1.59 GPa in the center of the island prior to delamination. These results are in excellent agreement with the experimentally observed critical island sizes for delamination and the typical values of film stress when this happens.

3.2. Axisymmetric analysis

In this section, we consider a circular island on a flat substrate and investigate the criterion for the nucleation and growth of an edge delamination crack under axisymmetric conditions. Following a similar approach adopted in the preceding section, we assume that the intercalation strain is large enough to cause sliding over the entire island. The radius of the island is denoted by R and the edge delamination crack considered here is an annular concentric ring whose front is located at distance a from the edge, as shown in Fig. 5. Treating the axisymmetric interfacial shear traction as a constant radial body force in the island and assuming that the deformation of the island can be described within plane stress approximation, the radial and tangential components of stresses in the film, at distance r from the center of island, can be obtained as (see Appendix A).

$$\sigma_{rr} = \frac{(2+\nu)}{3}\frac{\tau_0}{h}(R-a-r), \tag{10}$$

$$\sigma_{\theta\theta} = \frac{1}{3}\frac{\tau_0}{h}((2+\nu)(R-a)-(1+2\nu)r). \tag{11}$$

For the stress field given in Eqs. (10) and (11), the strain energy density u, within the region $R-a>r>0$, is calculated as[1]

$$u = \frac{\tau_0^2(1-\nu)}{18Eh^2}(2(2+\nu)^2(R-a)^2 - 6(1+\nu)(2+\nu)r(R-a) + (1+\nu)(5+4\nu)r^2). \tag{12}$$

The total elastic energy stored in the film is obtained by integrating u over the entire island, i.e. $U_{el} = \int_0^{R-a} 2\pi rhu\,dr$, which yields

$$U_{el} = \frac{\pi(1-\nu)(5+\nu)}{36}\frac{\tau_0^2}{Eh}(R-a)^4. \tag{13}$$

The elastic energy release rate is then

$$G = -\frac{dU_{el}}{da} = \frac{\pi(1-\nu)(5+\nu)}{9}\frac{\tau_0^2}{Eh}(R-a)^3. \tag{14}$$

The formation of the annular edge crack causes an increase in surface energy,

$$U_{surf} = \pi(R^2-(R-a)^2), \tag{15}$$

which grows at a rate of

$$\frac{dU_{surf}}{da} = 2\pi(R-a)\Gamma. \tag{16}$$

Using Eqs. (14) and (16), the Griffith condition for crack growth, i.e. $G > dU_{surf}/da$, gives

$$(R-a) > \sqrt{\frac{18Eh\Gamma}{(1-\nu)(5+\nu)\tau_0^2}}, \tag{17}$$

suggesting that crack nucleation in an initially crack-free interface is favorable only for islands larger than a critical size,

$$R > R_{cr,nuc} = \sqrt{\frac{18Eh\Gamma}{(1-\nu)(5+\nu)\tau_0^2}}. \tag{18}$$

Similar to Eq. (7), the crack would arrest when

$$a_{arr} = R - \sqrt{2R_{cr,nuc}^2 - R^2}. \tag{19}$$

Note this equation is valid as long as $R < \sqrt{2}R_{cr,nuc}$. For

$$R > R_{cr,del} = \sqrt{2}R_{cr,nuc}, \tag{20}$$

crack arrest is impossible and the edge crack would grow all the way to the center, leading to complete delamination.

For a 100 nm thick Si circular patch with $E = 40$ GPa and $\nu = 0.22$ [32], $\tau_0 \approx 10$ MPa [21,22] and $\Gamma = 1$ J/m^2, numerical estimates for the critical island sizes for nucleation and delamination by axisymmetric delamination are $2R_{cr,nuc} \approx 26.6$ μm and $2R_{cr,del} \approx 37.6$ μm, corresponding to maximum radial stresses of 0.98 and 1.39 GPa at the center of the island. Fig. 6a shows variations of the dimensionless elastic energy release rate and surface energy growth rate as a function of crack size. In this figure, $\tilde{U}_{el} = 18hEU_{el}/\pi(1-\nu)(5+\nu)\tau_0^2R^4$ and $\tilde{U}_{surf} = 18hEU_{surf}/\pi(1-\nu)(5+\nu)\tau_0^2R^4$ are dimensionless elastic and surface energies, respectively. As shown in this figure, at $a = 0$, corresponding to the case of no preexisting crack, the elastic energy release rate is equal to the rate of increase in

[1] In the analysis presented here, we have neglected the elastic energy stored in the delaminated part of the film for two reasons. First, we have carried out the full analysis that includes this part of the elastic energy and found no substantial changes in the results. Second, a delaminated thin membrane is susceptible to wrinkling which would cause part of the elastic energy to be released, bringing the solution closer to the present simplified analysis.

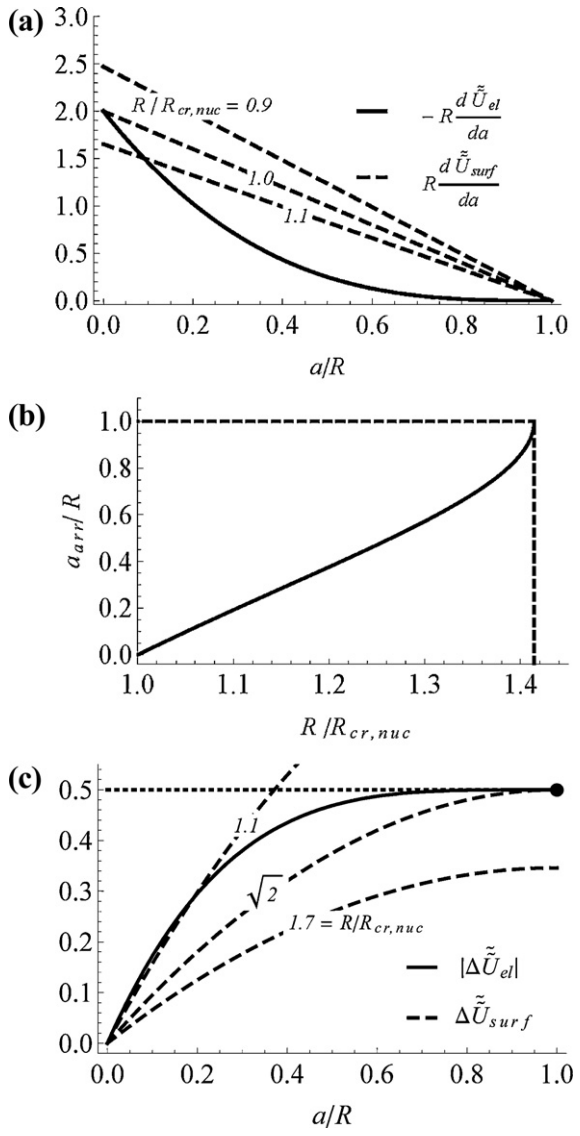

Fig. 6. Axisymmetric analysis of interfacial delamination of a circular Si island on substrate. (a) Elastic energy release rate and surface energy growth rate vs. crack length for various island sizes; (b) length of the arrested edge crack as a function of the island size; (c) changes in the elastic energy and surface energy as a function of the crack length for different island sizes.

surface energy when $R = R_{cr,nuc}$. When $R > R_{cr,nuc}$ ($R < R_{cr,nuc}$), the elastic energy release rate becomes larger (smaller) than the surface energy growth rate at $a = 0$, indicating that crack nucleation is energetically favorable (unfavorable), since it decreases (increases) the total free energy of the system.

Fig. 6b plots the dimensionless residual length of the arrested crack, a_{arr}/R, as a function of the dimensionless radius of the island $R/R_{cr,nuc}$. It can be seen from this figure that the length of the arrested crack would reach the radius of the island (i.e. $a_{arr} = R$) when $R = R_{cr,del} = \sqrt{2}R_{cr,nuc}$, corresponding to full delamination. Fig. 6c plots the changes in dimensionless elastic and surface energies, $|\Delta\tilde{\tilde{U}}_{el}| = \tilde{\tilde{U}}_{el}(0) - \tilde{\tilde{U}}_{el}(a)$ and $\Delta\tilde{\tilde{U}}_{surf} = \tilde{\tilde{U}}_{surf}(a) - \tilde{\tilde{U}}_{surf}(0)$, for islands of different sizes as a function of the crack length. It indicates that for an island with $R = R_{cr,del} = \sqrt{2}R_{cr,nuc}$, the total released elastic energy is just sufficient to drive the crack all the way to the center. This critical case has been marked by a solid circle in Fig. 6c. Further discussions are similar to the plane strain analysis.

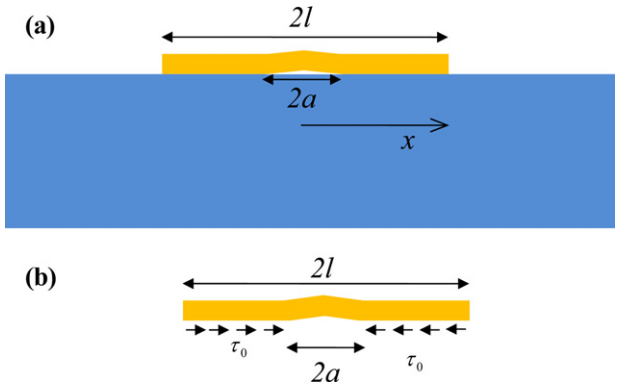

Fig. 7. Schematic of (a) a Si island on substrate with a center crack and (b) a free-body diagram of the island.

4. Analysis of center delamination cracks in the presence of large scale interfacial sliding

In this section, we consider interfacial cracks at the center of islands using a similar energy approach. Under the same assumptions as stated in Section 3, we consider the analysis under plane strain and axisymmetric conditions separately.

4.1. Plane strain analysis

Consider the same plane strain problem as in Section 3.1, but with an interface crack of length $2a$ located at the center of the island, as shown in Fig. 7. Under the same assumption of overlapping interfacial sliding zones, the normal stress in the film at distance x from the center of island can be written as

$$\sigma_{xx} = \frac{\tau_0}{h}\begin{cases} l-a & a > x > 0 \\ l-x & l > x > a \end{cases}. \tag{21}$$

It follows that the total elastic energy in half of the island is

$$U_{el} = \int_0^l \frac{(1-\nu^2)}{2E}\sigma_{xx}^2\, dx = \frac{(1-\nu^2)\tau_0^2}{6Eh}(l-a)^2(l+2a), \tag{22}$$

and the elastic energy release rate as

$$G = -\frac{dU_{el}}{da} = \frac{(1-\nu^2)\tau_0^2}{hE}a(l-a). \tag{23}$$

Note that the energy release rate vanishes at $a = 0$, indicating that a preexisting crack is needed for the crack growth condition $G > \Gamma$. This is in sharp contrast to the case of edge delamination where no preexisting cracks are necessary. As shown in the preceding section, even in an initially crack-free island, it is possible for an edge delamination crack to nucleate spontaneously. However, this is not the case for center cracks. To satisfy the growth condition, the length of the preexisting center crack a_0 should fall in the following range

$$a_{0,\max} > a_0 > a_{0,\min}, \tag{24}$$

where

$$a_{0,\min} = \frac{1}{2}l\left(1 - \sqrt{1 - \frac{4\Gamma Eh}{(1-\nu^2)\tau_0^2 l^2}}\right), \quad \text{and}$$

$$a_{0,\max} = \frac{1}{2}l\left(1 + \sqrt{1 - \frac{4\Gamma Eh}{(1-\nu^2)\tau_0^2 l^2}}\right).$$

The above equation breaks down for

$$\Gamma > \frac{(1-\nu^2)l^2\tau_0^2}{4Eh} \quad \text{or} \quad l < l_{cr}^* = \sqrt{\frac{4Eh\Gamma}{(1-\nu^2)\tau_0^2}}, \tag{25}$$

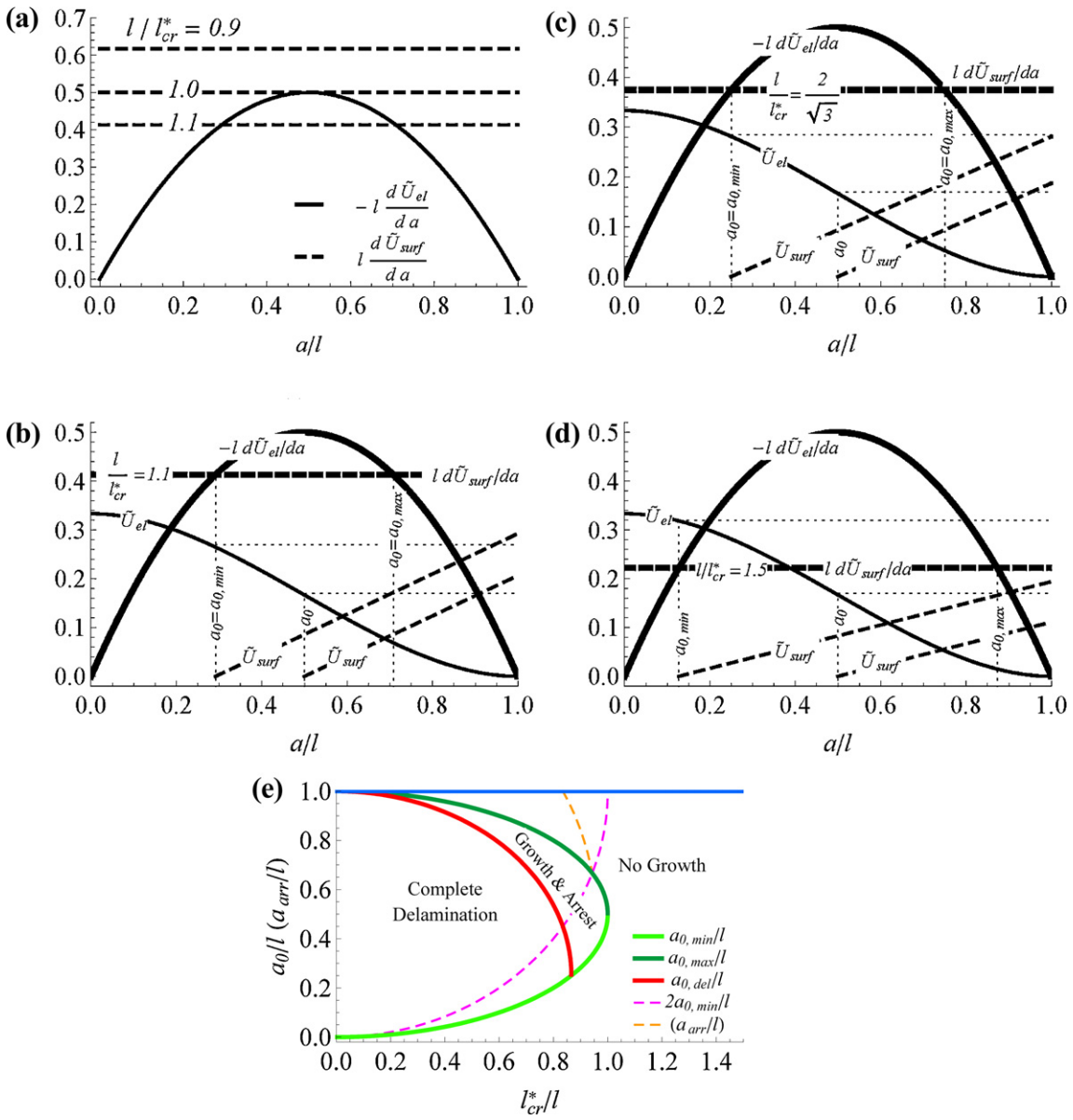

Fig. 8. Plane strain analysis of interfacial delamination of a Si island on substrate with a center crack at the interface: (a) elastic energy release rate and surface energy growth rate vs. crack length for various island sizes; total elastic energy of the island, total surface energy of the system and their changing rates associated with crack growth for (b) $l/l^*_{cr} = 1.1$, (c) $l/l^*_{cr} = 2/\sqrt{3}$, (d) $l/l^*_{cr} = 1.5$; (e) phase diagram indicating whether a preexisting crack will grow or not, and if so whether it will lead to full delamination, for given crack length and island size.

indicating that no center crack can grow, regardless of its length, when the island size is small enough. For the case of $l > l^*_{cr}$, a pre-existing crack of length $a_{0,\max} > a_0 > a_{0,\min}$ will grow. The crack will arrest when

$$U_{el}(a = a_0) - U_{el}(a = a_{arr}) = U_{surf}(a = a_{arr}) - U_{surf}(a = a_0), \tag{26}$$

where

$$U_{surf} = \Gamma(a - a_0), \tag{27}$$

is the surface energy of the system with respect to the initial state. Eq. (26) can be solved for a_{arr} to obtain

$$a_{arr} = \frac{1}{4}\left(3l - 2a_0 + \sqrt{9l^2 + 12a_0 l - 12a_0^2 - \frac{48\Gamma Eh}{(1-\nu^2)\tau_0^2}}\right). \tag{28}$$

By comparing a_{arr} with l, we can determine the condition for complete delamination. Bearing in mind the condition for crack growth, $a_{0,\min} < a_0 < a_{0,\max}$, complete delamination $a_{arr} > l$ requires

$$a_{0,\min} < a_0 < a_{0,del}, \tag{29}$$

where

$$a_{0,del} = \frac{1}{4}l\left(1 + \sqrt{9 - \frac{48\Gamma Eh}{(1-\nu^2)\tau_0^2 l^2}}\right). \tag{30}$$

This equation breaks down for

$$\Gamma > \frac{3(1-\nu^2)l^2\tau_0^2}{16Eh} \quad \text{or} \quad l < l^*_{cr,del} = \frac{2}{\sqrt{3}}l^*_{cr} = \sqrt{\frac{16Eh\Gamma}{3(1-\nu^2)\tau_0^2}}, \tag{31}$$

indicating that full delamination is impossible for sufficiently small islands. As expected, Eq. (25), which inhibits any crack growth, gives a stronger condition than Eq. (31), which allows growth but prevents full delamination. Fig. 8a shows variations of the

Table 1
Numerical estimates of the minimum length of the pre-existing crack required for full delamination for different island sizes based on the plane strain analysis.

	$l/l^*_{cr,del}$	1	1.34	1.67	2
Island size	$2l$ (μm)	29.95	40	50	60
	$a_{0,\min}$ (μm)	3.74	2.39	1.81	1.47
Max. stress	$\sigma_{\max}$ (GPa)	1.12	1.76	2.32	2.85

dimensionless elastic energy release rate as a function of the dimensionless crack length. As shown in this figure, the elastic energy release rate falls entirely below the rate at which the surface energy of the system increases for $l < l^*_{cr}$. However, for $l < l^*_{cr}$, these two curves intersect each other at two points corresponding to $a_{0,\min}$ and $a_{0,\max}$. The total elastic energy, the total surface energy, and their changing rate as a function of crack length are shown for various island sizes in Figs. 7b–d. In each of these figures, the surface energy curve has been plotted for two different preexisting crack lengths $a_0 = a_{0,\min}$, and $a_0 = 0.5l$. As shown in Fig. 8b for $l = 1.1l^*_{cr} < l^*_{cr,del}$, neither of these two preexisting cracks can grow all the way to the edge, as the elastic energy in the patch is not sufficient to drive full delamination, i.e. $U_{el}(a = a_0) - U_{el}(a = l) < U_{surf}(a = l) - U_{surf}(a = a_0)$. This is consistent with the critical condition for complete delamination given by Eq. (31). In the critical case of $l = (2/\sqrt{3})l^*_{cr} = l^*_{cr,del}$, shown on Fig. 8c, a preexisting crack with $a_0 = a_{0,\min} = 0.25l$ can grow all the way to the edge leading to complete delamination, as Eq. (26) is satisfied. In comparison, a preexisting crack with $a_0 = 0.5l$ is arrested when $U_{el}(a = a_0) - U_{el}(a = l) < U_{surf}(a = l) - U_{surf}(a = a_0)$. Fig. 8d shows the case of $l = 1.5l^*_{cr} > l^*_{cr,del}$, in which both of the preexisting cracks considered here grow all the way to the edge, leading to full delamination, as they satisfy $U_{el}(a = a_0) - U_{el}(a = l) > U_{surf}(a = l) - U_{surf}(a = a_0)$.

A summary of the analysis presented above can be cast in a phase-diagram shown in Fig. 8e. In this figure, the horizontal axis is a measure of the island size or interface toughness, and the vertical axis shows the length of the preexisting crack. Three regions have been indicated on this figure, which are separated by solid curves. Given the dimensionless length of the preexisting crack a_0/l and the dimensionless size of the island l^*_{cr}/l, the phase diagram indicates whether the crack can grow or not, and if it can, whether it will be arrested. The dashed curve labeled as "$2a_{0,\min}/l$" provides an example of the case of $a_0 = 2a_{0,\min}$. As shown in the figure, this curve goes through all three regions. For the segment of this curve which falls in the "Growth & Arrest" region, the length of the arrested crack has been shown by the dashed curve labeled as "(a_{arr}/l)", which can be read out from the vertical axis for a given l^*_{cr}/l.

For 100 nm thick Si islands with $E = 40$ GPa and $\nu = 0.22$ [32], $\tau_0 \approx 10$ MPa [21,22] and $\Gamma = 1$ J/m^2, the critical island sizes $2l^*_{cr}$ and $2l^*_{cr,del}$ are estimated to be 25.94 μm and 29.94 μm, respectively. The minimum length of the required pre-existing cracks for full delamination, and the corresponding maximum stresses in the film prior to crack growth, are given for different island sizes in Table 1. It should be noted that while the maximum stresses given in this table exceed the apparent flow stress observed in Si thin films (1–1.7 GPa) [33], our assumption of overlapping interfacial sliding in the island is not necessarily violated. This is because the latter is, in fact, an *averaged* flow stress while the actual stress distribution in the film is not uniform.

4.2. Axisymmetric analysis

In this section, we consider a central penny-shaped interfacial crack of radius a, as shown in Fig. 9. Invoking the same assumption of overlapping interfacial sliding zones as in the foregoing section,

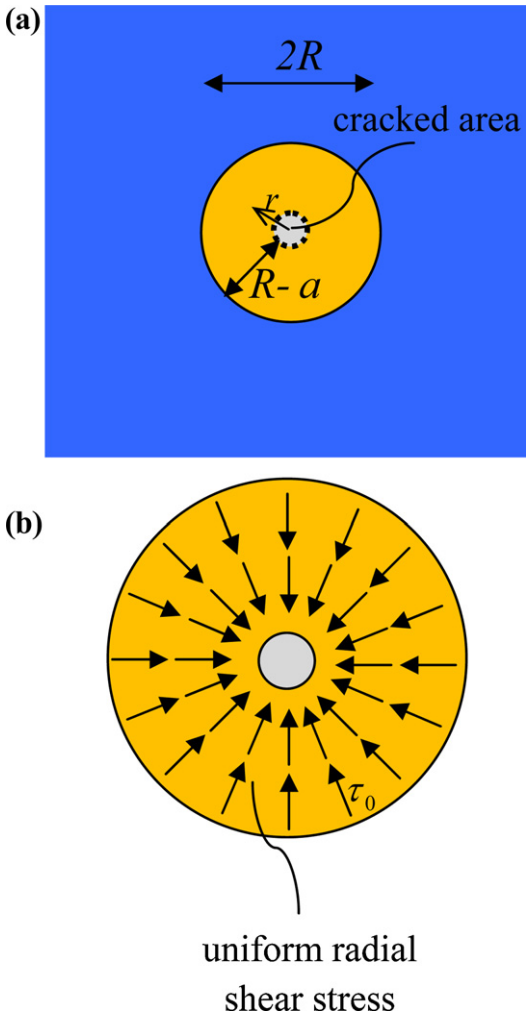

Fig. 9. Schematic of (a) a circular Si island on substrate with a penny-shaped center crack and (b) a free-body diagram of the island.

Appendix B shows that radial and hoop stresses within the patch can be expressed as

$$\sigma_{rr} = \frac{\tau_0}{6hR^2}\begin{cases} 2(2+\nu)R^3 - 3(1+\nu)R^2a - a^3(1-\nu) & a > r > 0 \\ (R-r)\left(2(2+\nu)R^2 + (1-\nu)\dfrac{a^3}{r^2}(R+r)\right) & R > r > a \end{cases}, \tag{32}$$

$$\sigma_{\theta\theta} = \frac{\tau_0}{6hR^2}\begin{cases} 2(2+\nu)R^3 - 3(1+\nu)R^2a - a^3(1-\nu) & a > r > 0 \\ 2(2+\nu)R^3 - 2(1+2\nu)rR^2 - (1-\nu)\dfrac{a^3}{r^2}(R^2+r^2) & R > r > a \end{cases}. \tag{33}$$

The total elastic energy of the patch can thus be calculated as

$$U_{el} = \frac{\pi(1-\nu)\tau_0^2}{36EhR^2}((5+\nu)R^6 - 8(2+\nu)R^3a^3 + 9(1+\nu)R^2a^4 + 2(1-\nu)a^6). \tag{34}$$

The elastic energy release rate is then

$$G = -\frac{dU_{el}}{da} = \frac{\pi(1-\nu)\tau_0^2}{3EhR^2}a^2(2R^3(2+\nu) - 3(1+\nu)R^2a - (1-\nu)a^3). \tag{35}$$

During crack growth, the surface energy associated with the crack,

$$U_{surf} = \pi(a^2 - a_0^2)\Gamma, \tag{36}$$

would grow at a rate of

$$\frac{dU_{surf}}{da} = 2\pi a\Gamma. \tag{37}$$

While the elastic energy release rate and its first derivative with respect to the crack length vanish at $a = 0$, dU_{surf}/da vanishes at

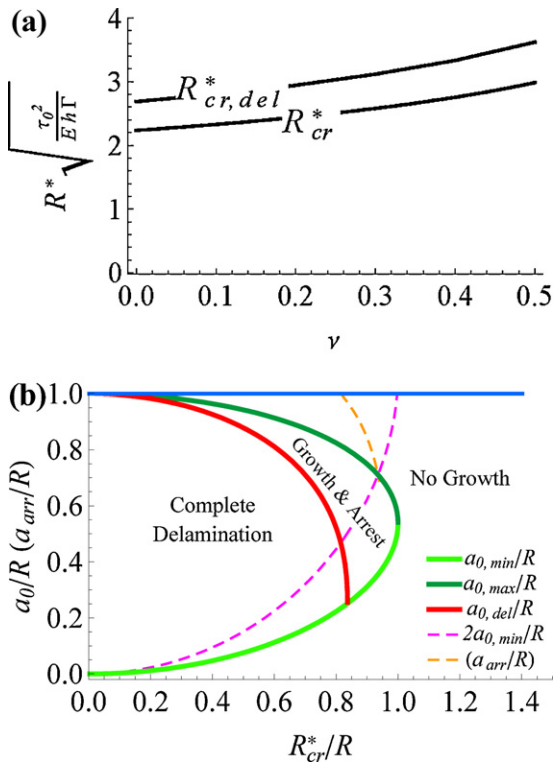

Fig. 10. Axisymmetric analysis of interfacial delamination of a circular island on substrate. (a) Critical length scales as a function of the Poisson's ratio of the island; (b) phase diagram in terms of preexisting crack length and island size.

$a=0$ but has a finite positive derivative with respect to a. Therefore $G<dU_{surf}/da$ in the vicinity of $a=0$, and similar to the plane strain case, cracking at the center is impossible without a preexisting crack. While essential features of this problem remain similar to the plane strain analysis presented before, the algebraic calculations become rather complicated since the elastic energy is a sixth order polynomial with respect to the crack length. The details of the analysis are skipped here and the emphasis is directed at the main findings. Similar to the plane strain case, we can identify two critical length scales R^*_{cr}, and $R^*_{cr,del}$. If the island radius falls below R^*_{cr}, no preexisting circular crack can grow, regardless of its radius, while if the island radius falls below $R^*_{cr,del}$, no preexisting crack can lead to complete delamination. These length scales as a function of the Poisson's ratio of the island are shown in Fig. 10a. For 100 nm thick Si islands with $E=40$ GPa and $\nu=0.22$ [32], $\tau_0\approx10$ MPa [21,22] and $\Gamma=1$ J/m^2, numerical estimates for the critical island sizes are $2R^*_{cr}\approx31.2$ μm and $2R^*_{cr,del}\approx37.6$ μm. The minimum length of the center cracks which leads to complete delamination, and the corresponding maximum stresses for different island sizes, are given in Table 2. A summary of the detailed analysis is presented in Fig. 10b, in the form of a phase diagram similar to the one presented for the plane strain case, for the case $\nu=0.25$.

Table 2
Numerical estimates of the minimum length of the pre-existing crack required for full delamination for circular islands of different sizes.

	$R/R^*_{cr,del}$	1	1.06	2.12	3.19
Island size	$2R$ (μm)	37.64	40	60	80
	$a_{0,\min}$ (μm)	4.63	4.20	2.48	1.80
Max. stress	$\sigma_{\max}$ (GPa)	1.11	1.22	2.06	2.85

5. Conclusion

In summary, we have proposed a method to deduce the critical size for interfacial delamination of patterned thin film electrodes on substrate in the presence of large scale interfacial sliding. We have investigated the critical conditions of interfacial delamination with plane strain and axisymmetric analysis of both edge and center delamination cracks at the interface between thin film islands and the substrate. Our analysis shows that the overlapping interfacial sliding zones due to the finite interfacial sliding strength lead to a new class of size effects in interfacial delamination. Interfacial delamination of the electrodes becomes impossible when the island size falls below a critical length scale. Applications to lithiation of thin-film Si islands give results in excellent agreement with the experimentally observed size effects. The present work provides insights for optimized structural design to mitigate the mechanical degradation in high-capacity electrodes.

Acknowledgement

The work is supported by the GM-Brown Collaborative Research Laboratory on Computational Materials Science.

Appendix A.

Consider a circular membrane of radius R_a, subject to a uniform mismatch strain ε^* and uniform radial shear stress τ_0. Deformation of the patch, within plane stress approximation and in the presence of interfacial shear traction as body-force per unit volume of the patch $b=\tau_0/h$, can be described by the following differential equation

$$\frac{\partial}{\partial r}\left[\frac{1}{r}\frac{\partial}{\partial r}(ru)\right]+\frac{b(1-\nu^2)}{E}=0, \tag{A1}$$

where u is the radial displacement. General solution to the differential Eq. (A1) can be written in the form:

$$u=Ar+\frac{B}{r}-\frac{1}{3}\frac{\tau_0(1-\nu^2)}{Eh}r^2, \tag{A2}$$

where A and B are constants to be determined from boundary conditions. Radial and hoop stresses in the patch are related to the displacement field via

$$\sigma_{rr}=\frac{E}{1-\nu^2}\left\{\frac{\partial u}{\partial r}+\nu\frac{u}{r}-(1+\nu)\varepsilon^*\right\}, \tag{A3}$$

$$\sigma_{\theta\theta}=\frac{E}{1-\nu^2}\left\{\nu\frac{\partial u}{\partial r}+\frac{u}{r}-(1+\nu)\varepsilon^*\right\}. \tag{A4}$$

Upon satisfying the boundary conditions, $u=0$ at $r=0$, and $\sigma_{rr}=0$ at $r=R_a$, the constants A and B are obtained as $A=\varepsilon^*+(1/3)\tau_0R_a(1-\nu)(2+\nu)/Eh$, $B=0$, and subsequently, the stress components are found as

$$\sigma_{rr}=\frac{\tau_0(2+\nu)}{3h}(R_a-r), \tag{A5}$$

$$\sigma_{\theta\theta}=\frac{\tau_0}{3h}((2+\nu)R_a-(1+2\nu)r)). \tag{A6}$$

Finally, Eqs. (10) and (11) can be reproduced by setting $R_a=R-a$.

Appendix B.

Consider a membrane of radius R, subject to a uniform shear stress τ_0 within the region $R>r>a$ and zero shear stress within

$a > r > 0$. In this case, the body-force in Eq. (A1) should be replaced by

$$b = \begin{cases} 0 & a > r > 0 \\ \dfrac{\tau_0}{h} & R > r > a \end{cases}. \tag{B1}$$

This equation can be solved within $R > r > 0$ to give

$$u = \begin{cases} A_1 r + \dfrac{B_1}{r} & a > r > 0 \\ A_2 r + \dfrac{B_2}{r} - \dfrac{1}{3}\dfrac{\tau_0(1-\nu^2)}{Eh} r^2 & R > r > a \end{cases}, \tag{B2}$$

where A_1, A_2, B_1 and B_2 are constants to be determined from boundary conditions $u = 0$ at $r = 0$, and $\sigma_{rr} = 0$ at $r = R_a$, and continuity conditions of the displacement as well as the radial stress at $r = a$. This yields

$$A_1 = \varepsilon^* - \frac{1}{6}\frac{\tau_0(1-\nu)}{Eh}(2R^3(2+\nu) - 3aR^2(1+\nu) - a^3(1-\nu)),$$

$$A_2 = A_1 + \frac{\tau_0 a(1-\nu^2)}{2Eh}, \quad B_1 = 0 \quad \text{and} \quad B_2 = \frac{-\tau_0 a^3(1-\nu^2)}{6Eh}..$$

Upon substitution of these constants in Eq. (B2), the radial and hoop stresses can be obtained from Eqs. (A3) and (A4), as given in Eqs. (32) and (33).

References

[1] U. Kasavajjula, C. Wang, A.J. Appleby, J. Power Sources 163 (2001) 1003.
[2] L.Y. Beaulieu, K.W. Eberman, R.L. Turner, L.J. Krause, J.R. Dahn, Electrochem. Solid-State Lett. 4 (2001) A137.
[3] S. Bourderau, T. Brousse, D.M. Schleich, J. Power Sources 81–82 (1999) 233.
[4] S.-J. Lee, J.-K. Lee, S.-H. Chung, H.Y. Lee, S.-M. Lee, H.-K. Baik, J. Power Sources 97–98 (2001) 191.
[5] J. Maranchi, A. Hepp, P. Kumta, Electrochem. Solid-State Lett. 6 (2003) A198.
[6] J. Graetz, C.C. Ahn, R. Yazami, B. Fultz, Electrochem. Solid-State Lett. 6 (2003) A194.
[7] J.P. Maranchi, A.F. Hepp, A.G. Evans, N.T. Nuhfer, P.N. Kumta, J. Electrochem. Soc. 153 (2006) A1264.
[8] I. Ryu, J.W. Choi, Y. Cui, W.D. Nix, J. Mech. Phys. Solids 59 (2011) 1717.
[9] X.H. Liu, et al., Nano Lett. 11 (2011) 3312.
[10] L.Q. Zhang, et al., ACS Nano 5 (2011) 4800.
[11] K.-L. Lee, J.-Y. Jung, S.-W. Lee, H.-S. Moon, J.-W. Park, J. Power Sources 129 (2004) 270.
[12] M.N. Obrovac, L. Christensen, Electrochem. Solid-State Lett. 7 (2004) A93.
[13] T.D. Hatchard, J.R. Dahn, J. Electrochem. Soc. 151 (2004) A838.
[14] T. Takamura, S. Ohara, M. Uehara, J. Suzuki, K. Sekine, J. Power Sources 129 (2004) 96.
[15] X. Xiao, P. Liu, M.W. Verbrugge, H. Haftbaradaran, H. Gao, J. Power Sources 196 (2011) 1409.
[16] L.B. Freund, S. Suresh, Thin Film Materials: Stress Defect Formation and Surface Evolution, second ed., Cambridge University Press, Cambridge, 2003.
[17] M.Y. He, A.G. Evans, J.W. Hutchinson, Acta Mater. 45 (1997) 3481.
[18] M.Y. He, A.G. Evans, J.W. Hutchinson, Phys. Status Sol. A 166 (1998) 19.
[19] H.H. Yu, M.Y. He, J.W. Hutchinson, Acta Mater. 49 (2001) 93.
[20] H.H. Yu, J.W. Hutchinson, Int. J. Fract. 113 (2002) 39.
[21] H. Haftbaradaran, S.K. Soni, B.W. Sheldon, X., Xiao, H. Gao, J. Appl. Mech., in press.
[22] S.K. Soni, B.W. Sheldon, X. Xiao, D. Ahn, M.W. Verbrugge, H. Haftbaradaran, H. Gao, J. Electochem. Soc. 159 (2012) A38.
[23] Q. Li, K.-S. Kim, Proc. R. Soc. A 464 (2008) 1319.
[24] R.A. Huggins, W.D. Nix, Ionics 6 (2000) 57.
[25] W.H. Woodford, Y.-M. Chiang, W.C. Carter, J. Electrochem. Soc. 157 (2010) A1052.
[26] T. Bhandakkar, H. Gao, Int. J. Solids Struct. 47 (2010) 1424.
[27] K. Zhao, M. Pharr, J.J. Vlassak, Z. Suo, J. Appl. Phys. 108 (2010) 073517.
[28] K. Zhao, M. Pharr, J.J. Vlassak, Z. Suo, J. Appl. Phys. 109 (2011) 016110.
[29] J. Li, A.K. Dozier, Y. Li, F. Yang, Y.-T. Cheng, J. Electrochem. Soc. 158 (2011) A689.
[30] T. Bhandakkar, H. Gao, Int. J. Solids Struct. 48 (2011) 2304.
[31] J. Shen, R. Raj, J. Power Sources 196 (2011) 5945.
[32] V.B. Shenoy, Y. Qi, P. Johari, J. Power Sources 195 (2010) 6825.
[33] A. Sethuraman, M.J. Chon, M. Shimshak, V. Srinivasan, P.R. Guduru, J. Power Sources 195 (2010) 5062.